



Raman-induced mode coupling in temporal waveguides formed by short solitonsJunchi Zhang ^{1,*}, William R. Donaldson,² and Govind P. Agrawal ^{1,2}¹*The Institute of Optics, University of Rochester, Rochester, New York 14627, USA*²*Laboratory of Laser Energetics, University of Rochester, Rochester, New York 14623-1299, USA*

(Received 30 December 2022; accepted 8 March 2023; published 21 March 2023)

We study the propagation of optical pulses trapped inside a temporal waveguide formed by two solitons in a dispersive nonlinear medium such as an optical fiber. The solitons are short enough that they decelerate as their spectra shift continuously toward the red side because of intrapulse Raman scattering. We show that the shape of a probe pulse trapped between the two solitons evolves in a periodic fashion, while its spectrum shifts toward the blue side. We develop a coupled-mode theory showing that such changes occur because of mode coupling induced by the deceleration of the short solitons, resulting in a curved waveguide. A simplified two-mode model is used to introduce a single-parameter governing modal coupling and to find the condition under which coupling becomes weak enough that the probe pulse blueshifts its spectrum without changes in its pulse shape.

DOI: [10.1103/PhysRevA.107.033512](https://doi.org/10.1103/PhysRevA.107.033512)**I. INTRODUCTION**

The interaction of optical pulses with a temporal boundary inside a dispersive medium has recently attracted considerable attention [1–6]. A temporal boundary is formed when the refractive index of the medium changes at a certain time. In the context of photon acceleration in plasmas [2,3], changes in the refractive index can be induced through an ionization front that creates a moving boundary. Such a moving boundary can also be produced using nonlinear optics. Sending a strong pump pulse through an optical fiber creates a moving boundary via the optical Kerr effect [4–6]. When such a boundary is formed inside a dispersive medium, a temporal analog of reflection occurs when a weak probe pulse interacts with the boundary [4]. When the index change is large enough, the probe pulse is totally reflected at this boundary, and its speed changes because of a large shift in its wavelength. This phenomenon has also been studied as an optical analog of the event horizon associated with a black hole [7–11].

Two moving boundaries that are separated in time can form a temporal waveguide that confines pulses to the time window created by the two boundaries [12]. Similar to a spatial waveguide, such a temporal waveguide has a set of modes with different shapes that propagate inside the temporal waveguide without any distortion.

If a pump pulse is used to create a moving temporal boundary within a nonlinear dispersive medium, its shape should not change much with propagation. One way to realize this is to ensure that the pump pulse propagates as a fundamental soliton in that medium. In the case of optical fibers, stable solitons form when pump pulses are not too short (width > 1 ps). The situation changes for femtosecond pump pulses because several higher-order phenomena affect such pulses,

the most important being the intrapulse Raman scattering [13], which slows down the soliton by redshifting its spectrum continuously. Such solitons are called Raman solitons. A probe pulse's interaction with a Raman soliton has been studied [14–16] and it was found that the probe pulse can be trapped by the Raman soliton. There have also been studies on trapping of weak pulses between two solitons, effectively forming a temporal waveguide [17–20].

When two Raman solitons are created by a pair of short identical pump pulses, separated in time by a fixed delay, they form a temporal waveguide that is different from the waveguides studied earlier [6]. Because of intrapulse Raman scattering, both Raman solitons slow down identically, and the temporal window associated with the waveguide shifts in time continuously. In this paper, we study the evolution of a trapped probe pulse in such a decelerating temporal waveguide. We show that this type of temporal waveguide is analogous to a spatial waveguide whose core is curved or bent. Similar to the spatial case, the bending leads to coupling among different modes of the waveguide. We show that a trapped probe pulse undergoes periodic changes in its shape resulting from mode coupling, while its spectrum blueshifts continuously to ensure that its speed matches the speed of pump pulses. We develop an analytic approach based on coupled-mode theory and show that its predictions agree well with the numerical results.

The paper is organized as follows: Sec. II introduces the numerical model used to simulate the propagation of probe pulses in a temporal waveguide formed by two Raman solitons. Section III solves the coupled pump-probe equations numerically and discusses the behavior of a probe pulse trapped inside the waveguide. In Sec. IV, a noninertial frame in which the waveguide appears stationary is introduced. Using this frame, a coupled-mode theory is developed in Sec. V. This theory is used in Sec. VI to discuss the special case in which only two low-order modes are coupled strongly. A parameter indicative of the strength of mode coupling is

*jzh156@ur.rochester.edu

introduced and the conditions under which mode coupling becomes negligible and the probe pulse evolves without changing its shape is found. The main conclusions are summarized in Sec. VII.

II. PUMP-PROBE EQUATIONS

We consider a single-mode optical fiber as an example of a dispersive nonlinear medium. The generalized nonlinear Schrödinger equation is known to provide an excellent model for propagation of short optical pulses in such a medium [13]:

$$\begin{aligned} \frac{\partial A}{\partial z} - \sum_{m \geq 2} \frac{i^{m+1}}{m!} \beta_m \frac{\partial^m A}{\partial t^m} \\ = i\gamma A(z, t) \int_{-\infty}^{\infty} R(t') |A(z, t - t')|^2 dt'. \end{aligned} \quad (1)$$

The electric field $E(z, t)$ is related to the slowly varying envelope $A(z, t)$ as

$$E(z, t) = \frac{1}{2}(A(z, t) \exp[i\beta(\omega_1)z - \omega_1 t] + \text{c.c.}), \quad (2)$$

where ω_1 is the pump's center frequency and $\beta(\omega_1)$ is the propagation constant at this frequency. The variable t is related to the actual time t_a as $t = t_a - \beta_1 z$ and $\beta_m = d^m \beta / d\omega^m$ is the m th-order dispersion parameter of the fiber at the frequency ω_1 . Also, γ is the nonlinear parameter and the nonlinear response function [13],

$$R(t) = (1 - f_R)\delta(t) + f_R h_R(t), \quad (3)$$

includes the Raman response through $h_R(t)$, and f_R is its fractional contribution to $R(t)$.

As discussed earlier, pump pulses need to propagate as fundamental solitons, and their wavelength should lie in the anomalous dispersion region of the fiber where $\beta_2 < 0$. To form a temporal waveguide, the probe-pulse's group velocity should be close to that of pump pulses [12]. Moreover, a probe pulse is reflected only if its wavelength lies in the region where $\beta_2 > 0$. These two conditions imply that the probe-pulse's frequency ω_2 should be on the opposite side of the zero-dispersion wavelength of the fiber such that its speed nearly matches that of the pump pulses. As an example, the zero-dispersion wavelength of a standard single-mode fiber is near 1310 nm. If we choose 1500 nm as the wavelength of pump pulses, the wavelength of probe pulse should be near 1145 nm.

Since the spectra of such pump and probe pulses are widely separated, it is reasonable to separate the envelopes of the pump and the probe pulses using

$$A(z, t) = A_1(z, t) + A_2(z, t) e^{i(\Delta\beta z - \Delta\omega t)}, \quad (4)$$

where $\Delta\omega = \omega_2 - \omega_1$ and

$$\Delta\beta = \beta(\omega_2) - \beta(\omega_1) - \beta_1(\omega_1)\Delta\omega. \quad (5)$$

We substitute this form of $A(z, t)$ into Eq. (1) and separate the terms falling in two distinct spectral regions. This allows us to obtain two coupled pump-probe equations in

the form

$$\begin{aligned} \frac{\partial A_1}{\partial z} - \sum_{m \geq 2} \frac{i^{m+1}}{m!} \beta_{m1} \frac{\partial^m A_1}{\partial t^m} \\ = i\gamma A_1(1 - f_R)(|A_1|^2 + 2|A_2|^2) \\ + i\gamma f_R A_1 \int_{-\infty}^{\infty} h_R(t') (|A_1|^2 + |A_2|^2)(z, t - t') dt', \end{aligned} \quad (6)$$

$$\begin{aligned} \frac{\partial A_2}{\partial z} - \sum_{m \geq 2} \frac{i^{m+1}}{m!} \beta_{m2} \frac{\partial^m A_2}{\partial t^m} \\ = i\gamma A_2(1 - f_R)(|A_2|^2 + 2|A_1|^2) \\ + i\gamma f_R A_2 \int_{-\infty}^{\infty} h_R(t') (|A_2|^2 + |A_1|^2)(z, t - t') dt', \end{aligned} \quad (7)$$

where we neglected the terms that lie outside the pump and probe spectral regions. Such terms originate mostly from four-wave mixing, and can be neglected when the underlying phase-matching condition is not satisfied.

We solve the preceding coupled pump-probe equations numerically with the split-step Fourier method [13]. In our simulations, we used the following functional form for the Raman response function [21]:

$$h_R(t) = (1 - f_b) \frac{\tau_1^2 + \tau_2^2}{\tau_1 \tau_2} e^{-t/\tau_2} \sin \frac{t}{\tau_1} + f_b \frac{2\tau_b - t}{\tau_b^2} e^{-t/\tau_b}, \quad (8)$$

with $\tau_1 = 12.2$ fs, $\tau_2 = 32$ fs, $\tau_b = 96$ fs, $f_b = 0.21$, and $f_R = 0.245$.

III. NUMERICAL SIMULATIONS

We consider the situation where the probe pulse is located in the middle of two identical pump pulses that form two Raman solitons inside an optical fiber. Mathematically, we solve the coupled pump-probe equation with the following input at $z = 0$:

$$A_1(0, t) = \sqrt{P_1} \left[\text{sech}\left(\frac{t - \Delta T/2}{T_1}\right) + i \text{sech}\left(\frac{t + \Delta T/2}{T_1}\right) \right], \quad (9)$$

$$A_2(0, t) = \sqrt{P_2} \exp\left(-\frac{t^2}{2T_2^2}\right), \quad (10)$$

where ΔT is the separation between the two pump pulses of width T_1 . Their peak power is chosen such that $P_1 = |\beta_{21}|/\gamma T_1^2$ corresponds to a fundamental soliton. The 90° phase shift between the two pump pulses is introduced to prevent any nonlinear interaction between them [13]. The probe pulse has a Gaussian shape and its width T_2 is chosen to be considerably larger than that of pump pulses. In contrast, peak power P_2 of the probe is much smaller compared to that of the pump pulses to prevent its influence on the pump pulse.

As a specific example, we choose $T_1 = 200$ fs, $T_2 = 1$ ps, and $\Delta T = 5$ ps. The width of probe pulse approximately matches the fundamental mode of the temporal waveguide formed by two pump pulses. The values of dispersion parameters, $\beta_{21} = -\beta_{22} = -13.4$ ps²/km and $\beta_{31} = \beta_{32} = 0.07$ ps³/km, correspond to a silica fiber pumped at 1500 nm. All dispersion terms higher than third order were

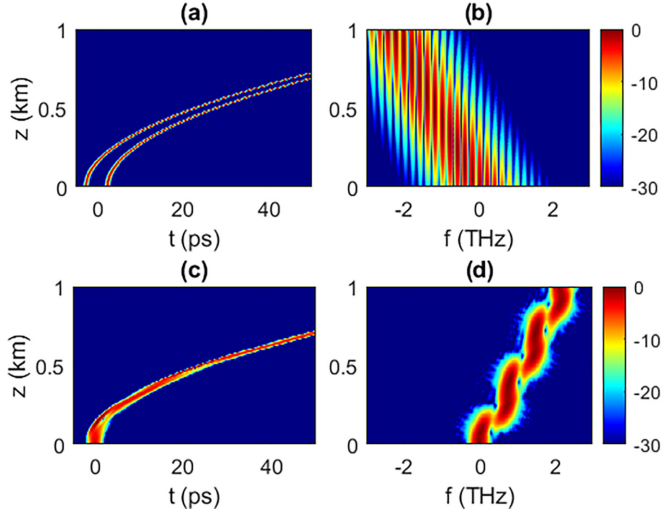


FIG. 1. (a), (c) Temporal and (b), (d) spectral evolutions of pump (top) and probe (bottom) pulses over a 1-km-long fiber. Probe pulse is trapped within the temporal waveguide formed by two Raman solitons. The intensity is plotted on a logarithmic (dB) scale.

neglected in our simulations. The nonlinear coefficient γ is 2 W km^{-1} .

Figure 1 shows the temporal and spectral evolution of the pump (top) and probe (bottom) pulses for a 1-km-long fiber. As expected, the spectrum of pump pulses continuously redshifts because of intrapulse Raman scattering. In the time domain, the trajectory of pump pulses is bent in a parabolic fashion because their deceleration caused by the spectral redshift produces a time delay varying as z^2 .

The evolution of the probe pulse in Fig. 1(c) shows clearly that it is trapped within the temporal waveguide formed by two solitons. In the absence of pump pulses, the probe's trajectory would be vertical, its spectrum would remain unchanged, and its width would increase because of dispersion. When the two pump pulses form a waveguide, the probe pulse is trapped between them and is forced to decelerate with them. In the spectral domain, the probe's spectrum shifts toward higher frequencies (a blueshift), and this shift is required for its speed to decrease. An interesting feature seen in Fig. 1(d) is that, although the pump's spectrum redshifts linearly with distance, the probe's spectrum does not do so. It exhibits a periodic evolution pattern in addition to the blueshift. In the time domain, the probe pulse also changes its shape in a periodic fashion. When the probe pulse collides with the soliton, it bounces back and its spectrum is shifted. This is the temporal reflection effect discussed in Ref. [4]. It can also be interpreted as the Doppler effect in a dispersive system. To understand the origin of these features, we develop a semianalytic approach in the next section. It reveals that the decelerating temporal waveguide is the temporal analog of a bent (or curved) spatial waveguide. The periodic spatial and temporal features result in both cases from coupling between the waveguide's modes induced by such bending.

IV. NONINERTIAL FRAME

The pump equation in Eq. (6) becomes decoupled from the probe equation when we neglect the terms containing

$|A_2|^2$ for weak probe pulses. If we also neglect the third- and higher-order dispersion terms, the pump equation can be solved approximately for pump pulses forming solitons [13]. Even though the soliton's shape does not change, its frequency and position change such that the solution has the form

$$A_1(z, t) = \sqrt{P_1} \left[\text{sech} \left(\frac{t - \Delta T/2 - q_p}{T_1} \right) + \text{isech} \left(\frac{t + \Delta T/2 - q_p}{T_1} \right) \right] e^{-i\Omega_p t + i\phi_p}, \quad (11)$$

where the Raman-induced frequency and temporal shifts are given by

$$\Omega_p = -\frac{8T_R|\beta_{21}|z}{15T_1^4}, \quad q_p = \frac{4T_R\beta_{21}^2 z^2}{15T_1^4} = az^2. \quad (12)$$

The parameter T_R has a value of about 3 fs found from the Raman response function [13]. The coefficient a , introduced using $q_p = az^2$, sets the quadratic delay of the pump pulse. The phase ϕ_p is not relevant for the following discussion.

Given the form in Eq. (11), it is beneficial to work in a noninertial frame in which the trajectory of pump solitons does not shift. This is done through the transformation

$$\tau = t - az^2. \quad (13)$$

In this frame, the temporal shape of each pump-pulse power does not change with z , i.e., $|A_1(z, \tau)|^2 = |A_1(0, \tau)|^2$. However, a new term appears in the probe Eq. (7):

$$\frac{\partial A_2}{\partial z} - 2az \frac{\partial A_2}{\partial \tau} + \frac{i}{2} \beta_{22} \frac{\partial^2 A_2}{\partial \tau^2} = ib(\tau)A_2, \quad (14)$$

where we kept only the dominant $m = 2$ dispersion term and defined $b(\tau)$ as

$$b(\tau) = 2\gamma(1 - f_R)|A_1(\tau)|^2 + \gamma f_R \int_{-\infty}^{\infty} h_R(\tau')|A_1(\tau - \tau')|^2 \times d\tau' \approx \gamma(2 - f_R)|A_1(\tau)|^2. \quad (15)$$

The approximate form of $b(\tau)$ holds for probe pulses considerably wider than pump pulses.

We use Eq. (14) in the next section to find the waveguide modes and to study the Raman-induced coupling among them. If the second term containing the parameter a is absent in this equation, its form becomes identical to the 1D Schrödinger equation, with z playing the role of time and $b(\tau)$ acting as the potential created by the pump pulses. The term containing a results from the use of a noninertial frame and its dependence on z makes the Hamiltonian “time dependent.” It perturbs a temporal waveguide such that its modes keep changing with z .

V. COUPLED-MODE EQUATIONS

We write Eq. (14) in the form of a Schrödinger equation as

$$-i \frac{\partial A_2}{\partial z} = \hat{H}(z)A_2(z, \tau), \quad (16)$$

where the Hamiltonian is given by

$$\hat{H}(z) = -\frac{\beta_{22}}{2} \frac{\partial^2}{\partial \tau^2} - 2iaz \frac{\partial}{\partial \tau} + b(\tau). \quad (17)$$

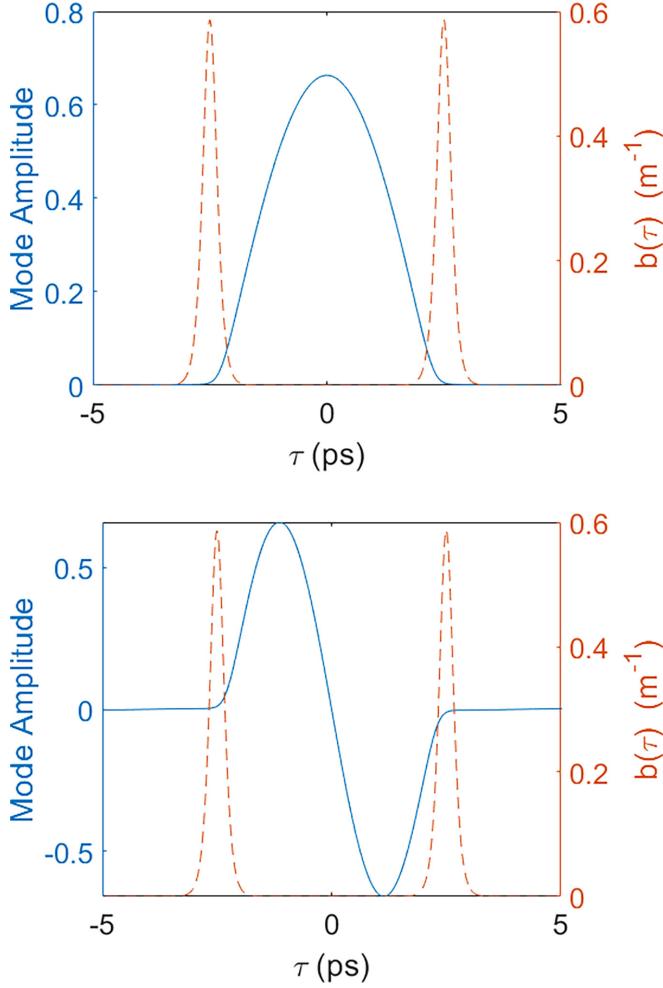


FIG. 2. First two modes of the temporal waveguide formed by two solitons with $T_1 = 0.2$ ps and $\Delta T = 5$ ps.

Recalling that z plays the role of time and τ that of a spatial coordinate, Eq. (16) shows that we are dealing with a time-dependent Hamiltonian. We can find the eigenmodes of this Hamiltonian for any value of z , but they will evolve with z . We adopt the approach used for a harmonic oscillator whose frequency varies with time [22].

Let $\psi_p(z, \tau)$ be the p th eigenmode of the Hamiltonian with the eigenvalue $\Delta\beta_p(z)$, i.e.,

$$\hat{H}(z)\psi_p(z, t) = \Delta\beta_p(z)\psi_p(z, t). \quad (18)$$

The eigenmodes at $z = 0$ can be found numerically using the same parameters as those in Fig. 1. The first- and second-order modes are shown in Fig. 2. The two modes resemble the eigenmodes of a quantum well because each soliton acts as a high-index barrier.

In Eq. (17), the second term containing az has its origin in the group-velocity mismatch between the pump and probe pulses. This mismatch can be compensated if the probe pulse shifts its frequency to match the group velocity of the pump. Based on this concept, the eigenmodes and eigenvalues of Eq. (18) at any distance z are found

to be

$$\psi_p(z, \tau) = \psi_p(0, \tau) \exp(-i2az\tau/\beta_{22}), \quad (19)$$

$$\Delta\beta_p(z) = \Delta\beta_p(0) - 2a^2z^2/\beta_{22}. \quad (20)$$

It is easy to conclude that the temporal shape of the eigenmodes does not change on propagation, but they undergo a frequency shift that increases linearly with the propagation distance. This shift has its origin in the linear redshift of pump pulses resulting from intrapulse Raman scattering. However, its sign is opposite to that of pump pulses, indicating that the mode frequencies shift toward the blue side.

Let us consider the situation in which a specific eigenmode, say $\psi_p(0, \tau)$, is excited at the input end of the temporal waveguide. If $\hat{H}(z)$ changes slowly enough that the adiabatic approximation holds, this mode will evolve to become $\psi_p(z, \tau)$ without coupling to other modes [22]. From Eq. (20), the mode shape will not change even though its frequency will shift toward the blue side.

In general, a probe pulse will excite multiple modes of the temporal waveguide, and its shape will change because of the coupling among different modes taking place during its propagation. To study this mode coupling, we decompose the probe pulse into the eigenmodes of $\hat{H}(z)$ as

$$A_2(z, \tau) = \sum_p C_p(z)\psi_p(z, \tau). \quad (21)$$

Using this expansion in Eq. (16), we obtain

$$\sum_p \frac{dC_p}{dz} \psi_p + \sum_p C_p \frac{\partial \psi_p}{\partial z} = i \sum_p C_p \Delta\beta_p \psi_p. \quad (22)$$

After decomposing $\partial \psi_p / \partial z$ in terms of the eigenmodes, we obtain the following evolution equation for the modal amplitudes [22]:

$$\frac{dC_p}{dz} + \sum_n d_{pn} C_n = i C_p \Delta\beta_p, \quad (23)$$

where $d_{pn} = \langle \psi_p | \partial \psi_n / \partial z \rangle$ is given by

$$d_{pn} = -\frac{2ia}{\beta_{22}} \int_{-\infty}^{\infty} \tau \psi_p^*(0, \tau) \psi_n(0, \tau) d\tau = -\frac{2ia}{\beta_{22}} T_{pn} \quad (24)$$

Noting that $\psi_p(0, \tau)$ is real, T_{pn} is defined as

$$T_{pn} = T_{np} = \int_{-\infty}^{\infty} \tau \psi_p(0, \tau) \psi_n(0, \tau) d\tau. \quad (25)$$

The last term in Eq. (23) can be eliminated with the transformation

$$C_p(z) = E_p(z) \exp \left[i \int_0^z \Delta\beta_p(z') dz' \right]. \quad (26)$$

In terms of E_p , the set of coupled-mode equations takes the form

$$\frac{dE_p}{dz} = \frac{2ia}{\beta_{22}} \sum_n T_{pn} e^{ib_{np}z} E_n, \quad (27)$$

where b_{np} is defined as

$$b_{np} = \Delta\beta_n(z) - \Delta\beta_p(z) = \Delta\beta_n(0) - \Delta\beta_p(0). \quad (28)$$

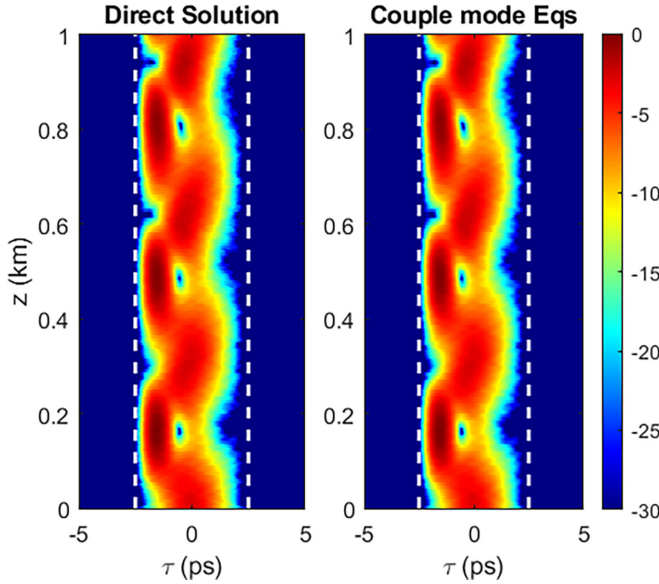


FIG. 3. Temporal evolution of probe pulse in the noninertial frame with the same parameter values used in Fig. 1. Left: Solution of Eq. (14). Right: Solution based on the coupled-mode equations in Eq. (27).

This set of relatively simple equations governs the Raman-induced coupling of the modes of a temporal waveguide. Notice that only the difference of initial eigenvalues at $z = 0$ appears in Eq. (28) because all eigenvalues change with z by the same amount in Eq. (20). Note that in this case, there is no geometrical phase because $T_{mn} = 0$ from the parity symmetry of the eigenmode.

Using the same parameter values used for Fig. 1, we simulated the probe-pulse propagation in the noninertial frame in two different ways. The results are shown in Fig. 3, where we plot the temporal evolution of the probe pulse in a 1-km-long fiber. On the left, we directly solved the wave equation given in Eq. (14). Results shown on the right were obtained by solving the coupled-mode equations in Eq. (27). In both cases, white dashed lines show the trajectories of the pump solitons that become vertical (no temporal shift) in the noninertial frame used here. The probe pulse, trapped between the two pump solitons, undergoes periodic changes in its shape, which become more apparent in the noninertial frame compared to the results shown in Fig. 1. The excellent agreement between the two approaches verifies the accuracy of our coupled-mode equations and justifies the approximations made in their derivation.

It should be apparent from Eq. (27) that $|E_p(z)|^2$ is a good measure of the fraction of energy of the probe pulse in a specific mode of the temporal waveguide at a distance z . Changes in the distribution of energy in different modes of the waveguide are shown in Fig. 4. As seen there, even though the first mode initially carries most energy at $z = 0$, coupling of this mode to higher-order modes leads to transfer of energy to other modes in a periodic fashion. This energy transfer manifests as periodic changes in the probe-pulse's shape in Fig. 3. However, the total energy of all the modes is conserved during the propagation. This is because the probe

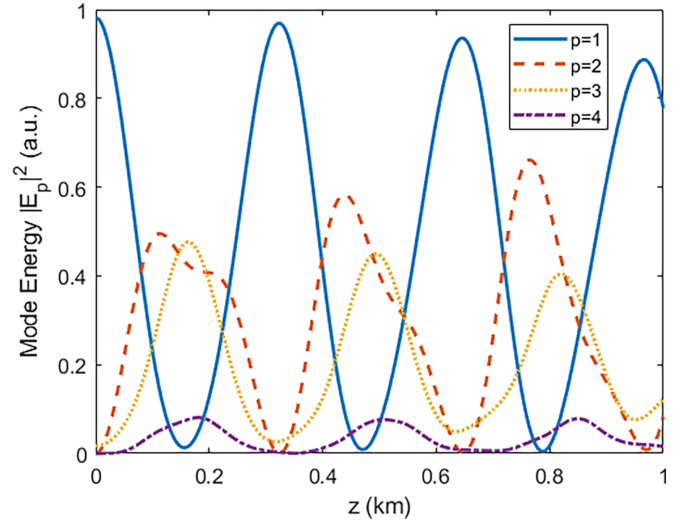


FIG. 4. Changes occurring with distance in the distribution of probe's energy among different modes. Parameter values are the same as in Fig. 1.

pulse remains trapped during propagation and there is no energy exchange between the pump and probe.

VI. MODEL BASED ON TWO MODES

Mode coupling is an undesirable feature for practical applications. For example, the blueshift of the probe's spectrum can be useful for frequency conversion applications. However, because of mode coupling, probe-pulse's spectrum does not shift to the blue side in a controlled fashion. In this section, we use the coupled-mode equations to find the conditions under which coupling of the fundamental mode to its neighboring modes can be largely suppressed. In this situation, a temporal waveguide can be used to shift the probe's spectrum toward the blue side in an adiabatic fashion.

We have seen in Sec. V that the evolution of a probe pulse is governed by a z -dependent Hamiltonian. When the Hamiltonian changes slowly with z , the fundamental mode evolves adiabatically without coupling to neighboring modes of the waveguide. Close to this adiabatic limit, mode coupling is relatively weak, and the fundamental mode should couple only to the second mode. This suggests that we can get considerable physical insight by considering only the first two modes in Eq. (27) and solving the following set of two coupled equations:

$$\frac{dE_1}{dz} = \frac{2ia}{\beta_{22}} T_{12} e^{ib_{21}z} E_2, \quad \frac{dE_2}{dz} = \frac{2ia}{\beta_{22}} T_{12} e^{-ib_{21}z} E_1. \quad (29)$$

The preceding equations are identical to those obtained for a directional coupler and can be solved easily because of their linear nature. Assuming that only the fundamental mode is excited at the input end, the energy in the second-order mode is found to be

$$|E_2(z)|^2 = |E_1(0)|^2 \left(\frac{4aT_{12}}{\beta_{22}K} \right)^2 \sin^2 \frac{Kz}{2}, \quad (30)$$

where

$$K = \sqrt{b_{21}^2 + (4aT_{12}/\beta_{22})^2}. \quad (31)$$

Similar to a directional coupler, the mode's energy oscillates with z with the period $L_p = 2\pi/K$ and becomes maximum in the middle of each period. Using Eq. (30), the maximum energy fractional energy in the second order mode is

$$\frac{|E_2(z)|_{\max}^2}{|E_1(0)|^2} = \frac{F}{1+F}, \quad (32)$$

where the parameter F is introduced as

$$F = (4aT_{12}/\beta_{22}b_{21})^2. \quad (33)$$

When a temporal waveguide is designed to ensure $F \ll 1$, almost all energy of the probe pulse remains in the fundamental mode, and the mode evolves in an adiabatic fashion. When F becomes close to 1, the fundamental mode does not evolve adiabatically. The two-mode model ceases to apply for $F > 1$ because coupling to higher-order modes cannot be ignored. For the results shown in Figs. 3 and 4, the estimated value of F is 6.5. It is evident that more than two modes should be included for such large values of F . The main conclusion is that the mode coupling can be made negligible by ensuring that $F \ll 1$.

The expression for F in Eq. (33) depends on T_{12} , whose value can be calculated from Eq. (25) but requires the mode profiles that must be obtained numerically. To estimate the values of F as simply as possible, we assume that pump pulses are so short compared to the probe pulse that we can treat the waveguide as a quantum well of width ΔT , surrounded by walls of infinite potentials. The eigenfunctions and eigenvalues of such a quantum well are known in an analytic form, and they can be used to find the parameters T_{12} and b_{21} in Eq. (33). The use of these parameters leads to the following expression for F :

$$F \approx 1.68 \times 10^{-4} T_R^2 \Delta T^6 / T_1^8. \quad (34)$$

We stress that Eq. (34) provides only a rough estimate of F and should be used only for a qualitative understanding. To estimate the numerical value of F for optical fibers, we use the $T_R = 3$ fs. F depends both on the widths and spacing of two pump pulses used as temporal boundaries. High powers of both of these parameters in Eq. (34) indicate that mode coupling is very sensitive to the values of both of them. To make F small, we need to either increase T_1 or decrease ΔT . Increasing T_1 decreases the Raman-induced redshift and reduces bending of the waveguide. In practice, the delay ΔT between the two pump pulses is easily controlled. Its lower values reduce the waveguide's width and increase the difference in eigenvalues of different waveguide modes.

As seen in Eq. (34), F varies as $(\Delta T)^6$. Therefore, decreasing ΔT by 50% should significantly suppress mode coupling for the situation shown in Fig. 4. We keep all other parameters the same but choose $\Delta T = 2.5$ ps and $T_2 = 0.5$ ps. The results are shown in Fig. 5. Temporal evolution of the probe pulse should be compared to that in Fig. 3. Clearly, distortion of the probe pulse is reduced considerably. Note also that the probe's spectrum shifts toward the blue much

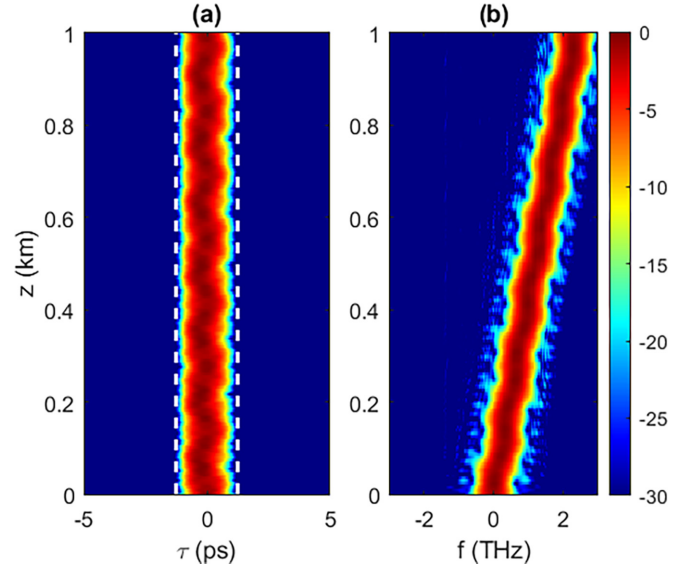


FIG. 5. (a) Temporal and (b) spectral evolution of a probe pulse ($T_2 = 0.5$ ps) inside a temporal waveguide with $\Delta T = 2.5$ ps.

more smoothly. The value of the parameter F is 0.0648 for the parameters used here. As $F \ll 1$, modal coupling should be relatively weak. This is indeed the case in Fig. 6, where the fractional energy of each mode is shown as a function of z using the coupled-mode equations. The fundamental mode dominates, and only a small fraction of its energy is transferred to the second mode in a periodic fashion. The results of the two-mode theory [Eq. (30)] agree well with the solution of the full coupled-mode equations [Eq. (27)] for such small values of F .

For completeness, we also consider the strong-coupling case by increasing the separation between the two pump pulses to 10 ps. The resulting temporal waveguide supports a large number of modes. The parameter F is 546 for this waveguide, indicating that mode coupling would lead to pulse distortion that is much more severe than that seen in Fig. 3. The results are shown in Fig. 7 for a probe pulse with $T_2 = 2$ ps. Coupling among a large number of modes severely

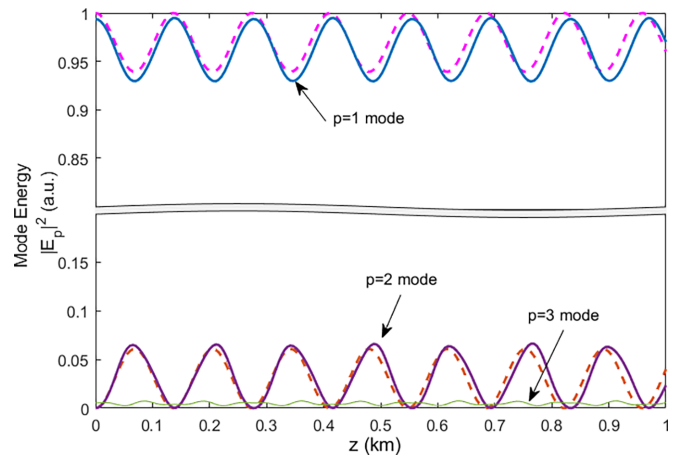


FIG. 6. Mode energies evolution in a 2.5-ps temporal waveguide in Fig. 5. Dashed lines show the result from two-mode theory.

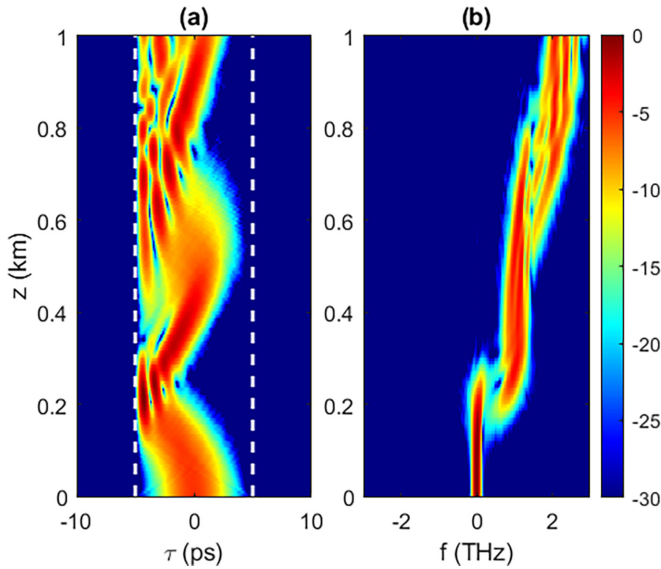


FIG. 7. (a) Temporal and (b) spectral evolution of a probe pulse ($T_2 = 2$ ps) inside a temporal waveguide with $\Delta T = 10$ ps.

distorts the shape of probe pulses, and the pulse's spectrum does not blueshift in a regular fashion.

VII. CONCLUSIONS

We have studied the propagation of optical pulses inside a temporal waveguide formed by two short pump-pulse solitons acting as high-index barriers. The wavelength of pump pulses is chosen such that they form solitons inside a dispersive nonlinear medium such as an optical fiber. The solitons are short enough that they decelerate as their spectra shift continuously toward the red side because of intrapulse Raman scattering. We show that the temporal waveguide formed by such solitons is not stationary, and the situation is analogous to a three-layer waveguide whose core is curved in space.

We use the coupled pump-probe equations to show that a probe pulse shifts its spectrum toward the blue side to match its speed with that of pump pulses so that it remains trapped inside such a temporal waveguide. However, the shape of the probe pulse evolves in a periodic fashion inside the waveguide. To understand this behavior, we make use of a noninertial reference frame for the probe pulse and find the eigenmodes and eigenvalues of the curved waveguide in this

frame. We use these modes to develop a set of coupled-mode equations, showing that shape changes occur because of mode coupling induced by the Raman-induced deceleration of pump solitons used to make the waveguide. A simplified two-mode model is used to introduce a single parameter governing modal coupling and to find the condition under which coupling becomes weak enough that the probe pulse blueshifts its spectrum without changes in its pulse shape.

From a practical standpoint, our study shows that the effects of stimulated Raman scattering must be considered when two femtosecond pump pulses with a fixed separation are employed to form a temporal waveguide that traps a probe pulse between the two pump pulses. The spectral blueshift of the probe pulse in such a waveguide can be useful for applications that require a tunable source of short pulses. It is difficult to change the wavelength of low-energy pulses. The technique used in this work transfers the Raman-induced redshift of pump pulses to probe pulses through cross-phase modulation as a blueshift, whose magnitude can be controlled by adjusting the width and spacing of pump pulses used to form the waveguide. It is worth noting that the mode coupling can also be induced through effects other than Raman scattering. As long as the speed of moving index boundary changes during propagation, temporal mode coupling would occur. For example, temporal mode coupling can be induced by tapering a waveguide.

ACKNOWLEDGMENTS

This work is supported by National Science Foundation (Grant No. ECCS-1933328), Department of Energy National Nuclear Security Administration (Grant No. DE-NA0003856), and New York State Energy Research and Development Authority.

This report was prepared as an account of work sponsored by an agency of the U.S. Government. Neither the U.S. Government nor any agency thereof, nor any of their employees, makes any warranty, express or implied, or assumes any legal liability or responsibility for the accuracy, completeness, or usefulness of any information, apparatus, product, or process disclosed, or represents that its use would not infringe privately owned rights. Reference herein to any specific commercial product, process, or service by trade name, trademark, manufacturer, or otherwise does not necessarily constitute or imply its endorsement, recommendation, or favoring by the U.S. Government or any agency thereof. The views and opinions of authors expressed herein do not necessarily state or reflect those of the U.S. Government or any agency thereof.

- [1] J. T. Mendonça and P. K. Shukla, Time refraction and time reflection: Two basic concepts, *Phys. Scr.* **65**, 160 (2002).
- [2] J. Dias, C. Stenz, N. Lopes, X. Badiche, F. Blasco, A. Dos Santos, L. O. e Silva, A. Mysyrowicz, A. Antonetti, and J. Mendonça, Experimental Evidence of Photon Acceleration of Ultrashort Laser Pulses in Relativistic Ionization Fronts, *Phys. Rev. Lett.* **78**, 4773 (1997).
- [3] J. T. Mendonça, *Theory of Photon Acceleration* (CRC Press, Bristol, 2000).
- [4] B. W. Plansinis, W. R. Donaldson, and G. P. Agrawal, What is the Temporal Analog of Reflection and Refraction of Optical Beams? *Phys. Rev. Lett.* **115**, 183901 (2015).
- [5] B. W. Plansinis, W. R. Donaldson, and G. P. Agrawal, Spectral splitting of optical pulses inside a dispersive medium at a temporal boundary, *IEEE J. Quantum Electron.* **52**, 6100708 (2016).
- [6] B. W. Plansinis, W. R. Donaldson, and G. P. Agrawal, Cross-phase-modulation-induced temporal reflection and waveguiding of optical pulses, *J. Opt. Soc. Am. B* **35**, 436 (2018).

- [7] T. G. Philbin, C. Kuklewicz, S. J. Robertson, S. Hill, F. König, and U. Leonhardt, Fiber-optical analog of the event horizon, *Science* **319**, 1367 (2008).
- [8] K. E. Webb, M. Erkintalo, Y. Xu, N. G. R. Broderick, J. M. Dudley, G. Genty, and S. G. Murdoch, Nonlinear optics of fibre event horizons, *Nat. Commun.* **5**, 4969 (2014).
- [9] A. Choudhary and F. König, Efficient frequency shifting of dispersive waves at solitons, *Opt. Express* **20**, 5538 (2012).
- [10] S. F. Wang, A. Mussot, M. Conforti, A. Bendahmane, X. L. Zeng, and A. Kudlinski, Optical event horizons from the collision of a soliton and its own dispersive wave, *Phys. Rev. A* **92**, 023837 (2015).
- [11] L. Tartara, Frequency shifting of femtosecond pulses by reflection at solitons, *IEEE J. Quantum Electron.* **48**, 1439 (2012).
- [12] B. W. Plansinis, W. R. Donaldson, and G. P. Agrawal, Temporal waveguides for optical pulses, *J. Opt. Soc. Am. B* **33**, 1112 (2016).
- [13] G. P. Agrawal, *Nonlinear Fiber Optics*, 6th ed. (Academic Press, Boston, 2019).
- [14] S. Robertson and U. Leonhardt, Frequency shifting at fiber-optical event horizons: The effect of Raman deceleration, *Phys. Rev. A* **81**, 063835 (2010).
- [15] A. V. Gorbach and D. V. Skryabin, Light trapping in gravity-like potentials and expansion of supercontinuum spectra in photonic-crystal fibres, *Nat. Photonics* **1**, 653 (2007).
- [16] J. Zhang, W. Donaldson, and G. P. Agrawal, Temporal reflection of an optical pulse from a short soliton: Impact of Raman scattering, *J. Opt. Soc. Am. B* **39**, 1950 (2022).
- [17] S. F. Wang, A. Mussot, M. Conforti, X. L. Zeng, and A. Kudlinski, Bouncing of a dispersive wave in a solitonic cage, *Opt. Lett.* **40**, 3320 (2015).
- [18] A. Shipulin, G. Onishchukov, and B. A. Malomed, Suppression of soliton jitter by a copropagating support structure, *J. Opt. Soc. Am. B* **14**, 3393 (1997).
- [19] Z. Deng, X. Fu, J. Liu, C. Zhao, and S. Wen, Trapping and controlling the dispersive wave within a solitonic well, *Opt. Express* **24**, 10302 (2016).
- [20] A. Demircan, S. Amiranashvili, C. Brée, U. Morgner, and G. Steinmeyer, Supercontinuum generation by multiple scatterings at a group velocity horizon, *Opt. Express* **22**, 3866 (2014).
- [21] Q. Lin and G. P. Agrawal, Raman response function for silica fibers, *Opt. Lett.* **31**, 3086 (2006).
- [22] J. J. Sakurai and J. Napolitano, *Modern Quantum Mechanics*, 3rd ed. (Cambridge University Press, Cambridge, 2021).